# Interannual to Decadal Variability in Climate and the Glacier Mass Balance in Washington, Western Canada, and Alaska*

C. M. BITZ

*School of Earth and Ocean Sciences, University of Victoria, Victoria, British Columbia, Canada*

D. S. BATTISTI

*Department of Atmospheric Sciences, University of Washington, Seattle, Washington*

(Manuscript received 20 February 1998, in final form 10 January 1999)

ABSTRACT

The authors examine the net winter, summer, and annual mass balance of six glaciers along the northwest coast of North America, extending from Washington State to Alaska. The net winter (NWB) and net annual (NAB) mass balance anomalies for the maritime glaciers in the southern group, located in Washington and British Columbia, are shown to be positively correlated with local precipitation anomalies and storminess (defined as the rms of high-passed 500-mb geopotential anomalies) and weakly and negatively correlated with local temperature anomalies. The NWB and NAB of the maritime Wolverine glacier in Alaska are also positively correlated with local precipitation, but they are *positively* correlated with local winter temperature and *negatively* correlated with local storminess. Hence, anomalies in mass balance at Wolverine result mainly from the change in moisture that is being advected into the region by anomalies in the averaged wintertime circulation rather than from a change in storminess. The patterns of the wintertime 500-mb circulation and storminess anomalies associated with years of high NWB in the southern glacier group are similar to those associated with low NWB years at the Wolverine glacier, and vice versa.

The decadal ENSO-like climate phenomenon discussed by Zhang et al. has a large impact on the NWB and NAB of these maritime glaciers, accounting for up to 35% of the variance in NWB. The 500-mb circulation and storminess anomalies associated with this decadal ENSO-like mode resemble the Pacific–North American pattern, as do 500-mb composites of years of extreme NWB of South Cascade glacier in Washington and of Wolverine glacier in Alaska. Hence, the decadal ENSO-like mode affects precipitation in a crucial way for the NWB of these glaciers. Specifically, the decadal ENSO-like phenomenon strongly affects the storminess over British Columbia and Washington and the moisture transported by the seasonally averaged circulation into maritime Alaska. In contrast, ENSO is only weakly related to NWB of these glaciers because (i) the large-scale circulation anomalies associated with ENSO do not produce substantial anomalies in moisture advection into Alaska, and (ii) the storminess and precipitation anomalies associated with ENSO are far to the south of the southern glacier group.

Finally, the authors discuss the potential for short-term climate forecasts of the mass balance for the maritime glaciers in the northwest of North America.

## 1. Introduction

Previous studies on the relationship between the local weather and the mass balance of glaciers in the maritime northwest of North America indicate that the annual changes in glacier mass balance are largely due to wintertime anomalies in accumulation, and the latter anomalies are mainly due to anomalies in precipitation with lesser contributions by anomalies in temperature (Letréguilly 1988). Anomalies in the summer ablation are only weakly correlated with the annual mass balance for maritime glaciers (Walters and Meier 1989).

Previous studies on the relationship between climate anomalies and the anomalies in the mass balance of the maritime glaciers of the northeastern Pacific have presumed the predominant climate anomalies to be the Pacific–North American (PNA) pattern, as defined in Wallace and Gutzler (1981) (e.g., Yarnal 1984; Walters and Meier 1989; Hodge et al. 1998), or by means of the PNA but initiated by the El Niño–Southern Oscillation (ENSO; e.g., Walters and Meier 1989; Hodge et al. 1998). The studies of Yarnal (1984) and Walters and Meier (1989) showed that the mass balance anomalies

* Joint Institute for the Study of the Atmosphere and Ocean Contribution Number 463.

*Corresponding author address:* Dr. C. M. Bitz, Quaternary Research Center, University of Washington, Box 351360, Seattle, WA 98195-1360.
E-mail: bitz@atmos.washington.edu

of the glaciers of the northeastern Pacific were indeed related to sea level pressure (SLP) anomalies resembling the PNA pattern.

Building on the early work on the PNA–ENSO relationship (Horel and Wallace 1981), in which extreme ENSO conditions in the Tropics were seen to be associated with anomalies in the PNA pattern, Walters and Meier (1989) postulated and found a weak relationship between ENSO and the glacier mass balance. Using longer data records, Hodge et al. (1998) also found a weak correlation between the glacier mass balance and ENSO, with the warm (cold) phase of ENSO being associated with positive (negative) winter mass balance anomalies on the glaciers in southeast Alaska (Washington and southern British Columbia). However, the relationship between ENSO and the PNA is weak, as is the relationship between ENSO and wintertime weather anomalies in the North American Pacific coast (e.g., see Cayan and Peterson 1989; see also Fig. 13 of Zhang et al. 1997). Hence, the link between ENSO and the glacier mass balance is also weak (Walters and Meier 1989). Hodge et al. (1998) echoed Walter and Meier's conjecture that PNA circulation anomalies in the midlatitude circulation were responsible for the ENSO–glacier relationship and that the anomalies in precipitation and mass balance were due to changes in the storm track, expressed by the PNA.

In this study, we reexamine the climatological factors that regulate the mass balance of the maritime glaciers in the northwest of North America, employing recent results that document an organized, large-scale climate phenomenon throughout the Pacific that occurs primarily on the decadal timescale and is referred to as the decadal ENSO-like variability whose index is known as the global residual (GR) index (e.g., Zhang et al. 1997). These decadal changes include anomalies throughout the Pacific that qualitatively resemble those associated with ENSO (Zhang et al. 1997). Other investigators have focused their work on the decadal variability in the midlatitude Pacific (e.g., Latif and Barnett 1994; Mantua et al. 1997), which has come to be known as the Pacific Decadal oscillation (PDO; Mantua et al. 1997). Crudely, the PDO is a combination of the midlatitude climate anomalies associated with ENSO and the decadal ENSO-like climate phenomena; the majority of the variance in the PDO is attributable to the Tropics (see sections 2 and 5).

In this paper, we demonstrate that, in contrast to ENSO, the decadal ENSO-like climate phenomenon has a profound effect on the mass balance of the maritime glaciers in Washington, British Columbia, and Alaska, accounting for up to 35% of the variance in the annual mass balance of the glaciers examined. The mass balance anomalies associated with this climate phenomenon are related to changes in the wintertime atmospheric circulation and, in a rather surprising fashion, to changes in the storm track in the northeast Pacific. Also in this study, we reexamine the weather processes that are responsible for the weak ENSO–glacier relationship, arriving at a very different scenario from that hypothesized in previous studies.

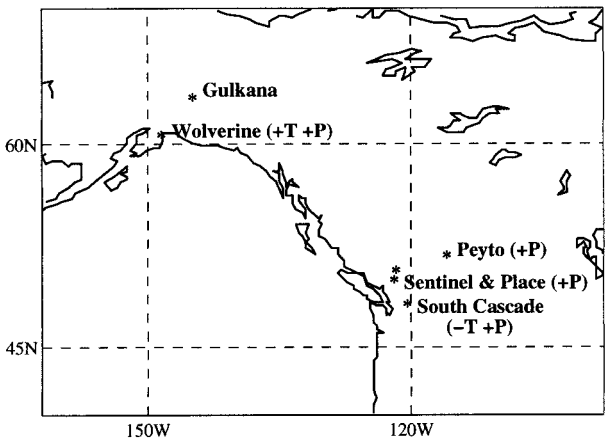


FIG. 1. Glacier locations are indicated by asterisks. Local wintertime climate variables that are found to be significantly correlated with anomalies in the net annual mass balance (NAB; section 3a) are indicated by P (precipitation) and T (temperature). Plus and minus signs indicate the sign of the correlation between climate variables and NAB.

## 2. Datasets and methodology

Six glaciers along the northwestern coast of North America were used for this study based on the availability of mass balance data segmented by winter and summer phases over several decades. The locations and names of the glaciers are shown in Fig. 1 and Table 1. Data from glaciers in the United States are provided by the U.S. Geological Survey. Glacier mass balance data used in this study are published in the *Fluctuations of Glaciers 1985–1990* (and previous volumes; Haeberli and Hoelzle 1993) and in the *Glacier Mass Balance Bulletin 1994–1995* (and previous issues; Haeberli et al. 1996).

There are several definitions by which the changes in a glacier's mass are measured. Measurements of the mass balance for the South Cascade, Sentinel, Place, and Peyto glaciers were made using the stratigraphic system; the mass balance data for Wolverine and Gulkana were obtained using the water cycle, or fixed year, system. Under the stratigraphic system, net mass balance (NB) is the net change in the mass of a glacier at the end of the ablation season, relative to the previous year. Under this system, the net mass balance can be broken down into winter and summer phases, where the winter mass balance (WMB) is the mass increase at the end of the accumulation season and the summer mass balance (SMB) is defined as the difference between NB and WMB. Hence, under this system the length of a season and the duration of a ''mass balance year'' varies from year to year. A second way to record mass balance is to make measurements at fixed times of the year,

TABLE 1. (top) A list of the glacier locations (from Table 1 in Walters and Meier 1989). (bottom) A list of the climate indexes used in this study (see section 2). Sources of glacier mass balance data are the U.S. Geological Survey (USGS) and the *Fluctuations of Glaciers* (FOG) serial.

| Glacier | Latitude | Longitude | Altitude range (m) | Period used | Source |
|---|---|---|---|---|---|
| South Cascade | 48°22′ | 121°3′W | 1600–2100 | 1959–95 | USGS |
| Sentinel | 49°54′ | 122°59′W | 1550–2100 | 1966–89 | FOG |
| Place | 50°25′ | 122°35′W | 1800–2600 | 1965–89 | FOG |
| Peyto | 51°40′ | 116°33′W | 2100–3200 | 1966–89 | FOG |
| Wolverine | 60°24′ | 148°55′W | 400–1700 | 1966–95 | USGS |
| Gulkana | 63°15′ | 145°25′W | 1200–2500 | 1966–95 | USGS |

| Climate index | Definition |
|---|---|
| CT | A reliable index of ENSO. The SST averaged from 6°N to 6°S, 180°W to 90°W, and then high-pass filtered to remove frequencies below 5 yr. |
| GR | An index of decadal ENSO-like variability. The expansion coefficient of the leading EOF of global ocean SST, after a linear fit to the CT time series is removed from the SST at each grid point. |
| PDO | An index including both ENSO and ENSO-like variability. The expansion coefficient of the leading EOF of SST poleward of 20°N in the Pacific Ocean. |

which are chosen to be consistent with the water cycle year. Under this measurement system, the net annual accumulation (AAc) and net annual ablation (AAb) are recorded to arrive at the net annual balance (AB), where annual is defined as the average over the water cycle year (i.e., from October to September). The AB and NB are not equivalent variables.[1] However, for our purposes we will neglect the difference and henceforth refer to both the AB and the NB as the net annual mass balance (NAB). The WMB and the AAc will be referred to as the net mass balance change over winter [net winter mass balance (NWB)]. Finally, the SMB and the AAb will be referred to as the net mass balance change over summer [net summer mass balance (NSB)]. The time-series of NAB, NWB, and NSB are shown in Fig. 2.

The locations and sources of meteorological station data used in this study are listed in Table 2. These stations were chosen for their proximity to glaciers and the length of their records. For the period 1966–95, Kenai River streamflow at Cooper Landing, Alaska, is used to corroborate the Alaskan precipitation. Runoff from the Kenai Mountains, where Wolverine glacier is located, contributes to the Kenai River streamflow.

We use gridded 500-mb height fields ($Z_{500}$) north of 30° latitude for the period 1947–94, taken from the National Centers for Environmental Prediction operational analysis (Kushnir and Wallace 1989). From this data, we calculate monthly maps of ''storminess'' as follows. At each grid point, the daily $Z_{500}$ anomalies are high-pass filtered in time using a binomial filter with weights [1 4 10 4 1]/16, as in Rogers (1997), to select variability in the 2–8-day range. Next, the root-mean-square (rms) of the filtered data is computed for each month, yielding a map of the monthly mean storminess.

The sea surface temperature (SST) data used to calculate the large-scale climate indexes, the cold tongue (CT), GR, and PDO (Table 1), were derived from an updated version of the U.K. Meteorological Office Historical SST dataset for 1900–93 (extended through 1996 with Optimally Interpolated SST from Reynolds and Smith 1995).

The CT index is the monthly mean SST anomaly averaged over the central and eastern equatorial Pacific (6°S–6°N, 180°–90°W) and represents the ENSO variability, which is predominately on interannual timescales. The index CT is closely related to Niño 3 and 4 and is perhaps the most reliable index of ENSO (Deser and Wallace 1990). Following Zhang et al. (1997), a 5-yr high-pass filter of the CT index is used in this study to isolate the interannual ENSO signal (Fig. 3).

We employ a second SST index, the GR, which is the expansion coefficient of the leading empirical orthogonal function (EOF) of global ocean SST, with a linear fit to the CT time series for 1904–90 removed from the expansion coefficient. Patterns of global climate anomalies associated with the GR index are found by regressing the GR index on the global fields of the SST, wind stress, and SLP (Fig. 4). Positive GR index is associated with warm (cold) water anomalies in the equatorial (northern) Pacific Ocean, anomalous westerly surface wind in the Tropics and in the storm track region, and high pressure and warm air anomalies over northern North America; the symmetry about the equator hints at the equatorial origin of the GR anomalies. The GR index (see Fig. 3) has lower-frequency variability than the CT, and there are marked jumps in the time series (e.g., 1940, 1976, and 1989). A complete description of this index is given in Zhang et al. (1997). The patterns associated with the GR time series displayed in Fig. 4 are decidedly similar to the patterns associated with ENSO: anomalies in SST, SLP, surface wind, and upper-level atmospheric circulation (e.g., the $Z_{500}$) are found

[1] Walters and Meier (1989) have a more complete presentation of the differences between these two measurement systems.

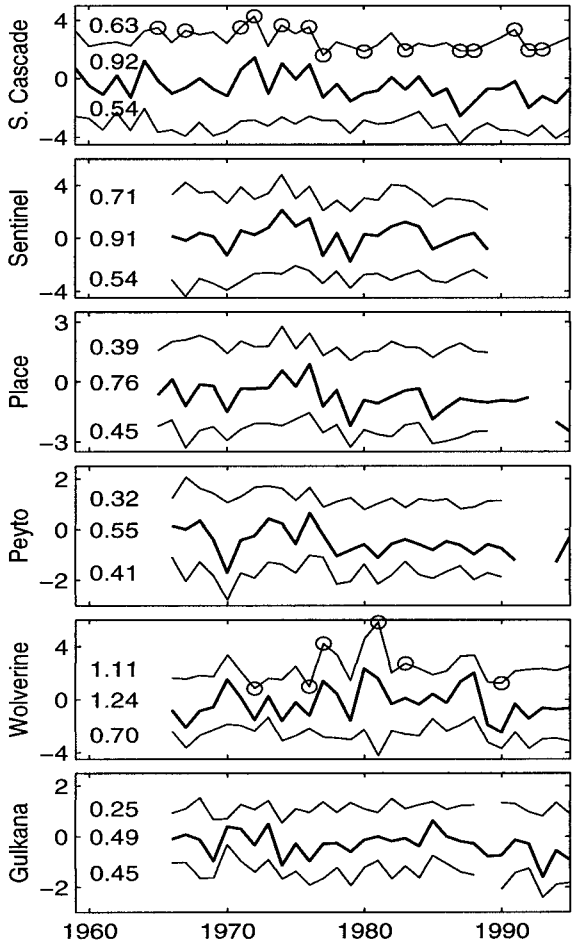


FIG. 2. Mass balance for the six glaciers used in this study: South Cascade, Sentinel, Place, Peyto, Wolverine, and Gulkana. In each panel, the NAB, ≈ net annual accumulation minus net annual ablation, is the heavy solid line. The thin solid lines that bracket each NAB curve denote the net mass balance change over the winter (NWB, upper line) and summer (NSB, lower line) seasons. The data are aligned along the abscissa such that, e.g., NAB (1980) = NWB (1980) + NSB (1980), where NWB (1980) spans the period fall 1979–spring 1980, NSB (1980) spans late spring and summer of 1980, and NAB (1980) spans fall 1979 to the end of summer 1980. Standard deviations of each time series are shown on the left side of the curve. Units are in meters of liquid water equivalent. Breaks in the curve indicate missing data. For the South Cascade and Wolverine glaciers, anomalies in NWB greater than one standard deviation above and below the mean are denoted with circles (see section 3b).

TABLE 2. Sources of precipitation and temperature station data include the National Oceanographic and Atmospheric Administration (NOAA), reports archived by the Washington state climatologists, the Global Historical Climatology Network (GHCN; Karl et al. 1990), and the U.S. Geological Survey (USGS). Where possible, time series have been extended beyond 1990 with data from the World Meteorological Organization.

| | Southern Alaskan stations | | | | |
|---|---|---|---|---|---|
| Name | Lat | Long | Elevation (m) | Period used | Source |
| Anchorage | 61°,10′N | 150°,01′W | 35 | 1959–93 | GHCN |
| Wolverine | 60°,24′N | 148°,55′W | 990 | 1967–95 | USGS |
| Gulkana | 62°,9′N | 145°,27′W | 479 | 1959–90 | GHCN |
| | Western Washington stations | | | | |
| Name | Lat | Long | Elevation (m) | Period used | Source |
| Quillayute | 48°,0′N | 124°,36′W | 55 | 1966–93 | NOAA |
| Seattle | 47°,36′N | 122°,30′W | 137 | 1959–94 | NOAA |
| Stampede | 47°,17′N | 121°,20′W | 1206 | 1959–94 | NOAA |
| Stevens Pass | 47°,44′N | 121°,05′W | 1241 | 1959–94 | NOAA |
| Paradise | 46°,47′N | 121°,44′W | 1654 | 1959–95 | NOAA |
| | Western Canadian stations | | | | |
| Name | Lat | Long | Elevation (m) | Period used | Source |
| Vancouver | 49°,12′N | 123°,12′W | 3 | 1959–93 | GHCN |
| Shalalth | 50°,44′N | 122°,13′W | 244 | 1963–90 | GHCN |
| Calgary | 51°,7′N | 114°,1′W | 1084 | 1959–93 | GHCN |
| Jasper | 52°,52′N | 118°,4′W | 1061 | 1959–93 | GHCN |

throughout the Pacific Ocean region and extend over the North American continent. However, there are subtle differences between the circulation anomalies over the North Pacific associated with the GR and CT time series (see Fig. 5), and we will see in section 4 that these differences are important for understanding the mass balance of the maritime glaciers of the northwest coast of North America.

The third SST index, the PDO, is the principle component of the leading eigenvector of SST poleward of 20°N in the Pacific Ocean (Mantua et al. 1997). In section 5, we show that much of the PDO is due to forcing from the tropical Pacific by the combined ENSO and decadal ENSO-like mode. Indeed the PDO is highly correlated with the GR ($r = 0.60$ for monthly and $r = 0.73$ for winter-averaged anomalies, over the period 1904–90). Our results will also show that the glacier mass balance is more highly correlated with PDO than with the GR. However, we argue in section 5 that the additional information in the PDO is likely to be associated with local climate variability that is unpredictable. Hence our calculations will use both the GR and PDO indexes.

## 3. Relationship between atmospheric circulation anomalies and the anomalies in the climate and glacier mass balance in the Pacific Northwest and Alaska

It is often argued that variability in the mass balance of maritime glaciers is dominated by the winter season precipitation, while continental glaciers are most strongly influenced by changes in the temperature during the summer season (see, e.g., Walters and Meier 1989). The relative standard deviation of NWB and NSB shown in Fig. 2 confirms this idea since the standard deviation of NWB at three coastal glaciers exceeds that of the NSB

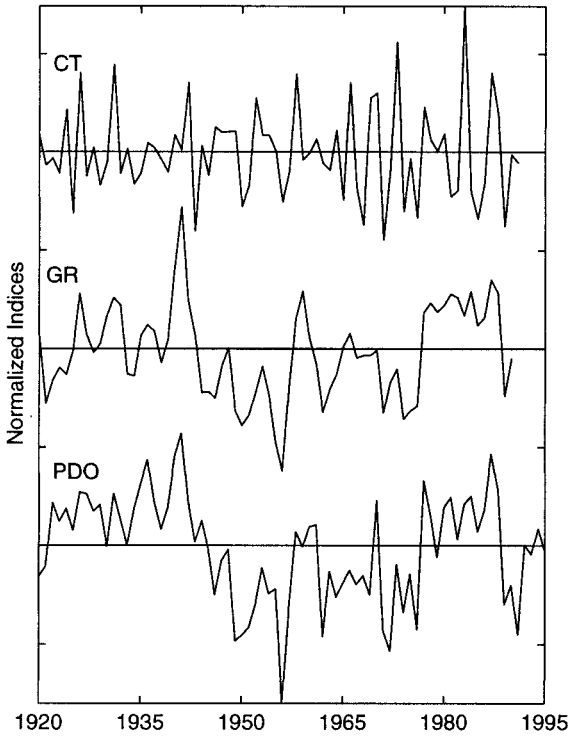


FIG. 3. Winter averaged values of the SST indexes. The plotting convention is such that, e.g., a datum plotted as 1954 is an average from Nov 1953 through Apr 1954.

and the reverse is true for Peyto and Gulkana, the two continental glaciers. Place glacier, located 200 km inland in the British Columbia coastal range, is intermediate between these two extremes.

It is also thought that there is a tendency for the NWB and NSB to be correlated, apparently because higher than normal accumulation during winter causes enhanced shortwave reflectivity during the summer season, resulting in less ablation. Among the six glaciers analyzed here, the only significant correlation between NWB and NSB, barely exceeding the 95% confidence level, occurs at Place glacier.

### *a. Mass balance dependence on the local temperature and precipitation*

We next examine the relationship between the glacier mass balance and the temperature and precipitation measured at nearby meteorological stations to diagnose the processes that are responsible for anomalies in the net winter mass balance for each glacier. We then examine the relationship between NWB and anomalies in the height of the wintertime mean 500-mb field ($Z_{500}$) and the anomalies in the storminess. Unless noted otherwise, we average the meteorological data over the boreal winter (November–April) and summer (May–October) seasons, respectively.

The anomalies in the South Cascade NWB are positively and highly correlated with local wintertime precipitation anomalies and negatively correlated with temperature (see Table 3). Anomalies in the NWB of the three Canadian glaciers are also positively correlated with anomalies in the wintertime precipitation at nearby stations (see Table 4; Letréguilly 1988; Demuth and Keller 1997). However, the NWB at Sentinel and Place glaciers is not significantly correlated with local temperature, and the correlation of NWB at Peyto glacier with local temperature is only marginally significant.[2] Moore and McKendry (1996) also found that the dominant climatological variable related to glacier mass balance in British Columbia is precipitation, although temperature was also important in the far southern part of the province. Finally, there is no statistically significant correlation between precipitation and temperature at any of the low-elevation Canadian and Washington stations (not shown), which suggests that temperature anomalies influence the NWB of the South Cascade and Peyto glaciers independently of changes in precipitation.

The relationships between the NWB and local precipitation and temperature at the Alaskan Wolverine glacier are very different compared to that at the Washington and western Canadian glaciers. In contrast to the South Cascade, Sentinel, Place, and Peyto glaciers (Tables 3 and 4), an anomalously large accumulation on the Wolverine glacier is associated with *positive* temperature anomalies in southern Alaska (Table 5; see also Mayo and Trabant 1984). NWB at the Wolverine glacier is significantly correlated with precipitation measured at the meteorological station on the glacier but not with precipitation measured at the other stations in Table 5. Mayo and March (1990) report that NWB at Wolverine is also positively correlated with precipitation measured at Seward, Alaska (at 40-m elevation). Furthermore, the correlation between Wolverine NWB and the winter–spring (November–June) streamflow of the nearby Kenai River is 0.80, suggesting that precipitation anomalies are indeed an important component in the variability of the NWB at Wolverine. (Streamflow anomalies cannot be predominately due to winter temperature anomalies that influence wintertime snow melt; otherwise, we would expect streamflow to be negatively correlated with NWB.) Hence we speculate that the Anchorage and Gulkana precipitation data are too regionally dependent or of poor quality, or that the records are too short, to yield information about Wolverine NWB.

Anomalies in the mass balance of the Gulkana glacier, located 350 km inland, do not seem to be associated with the same environmental anomalies as those that affect the mass balance of the Wolverine glacier. NWB at the continental Gulkana glacier does not depend sig-

[2] Letréguilly (1988) found that the correlation between the Peyto NWB and the temperature measured at nearby meteorological stations was higher for Jasper than for stations closer to Peyto, which she speculated was due to the duration and quality of the data.

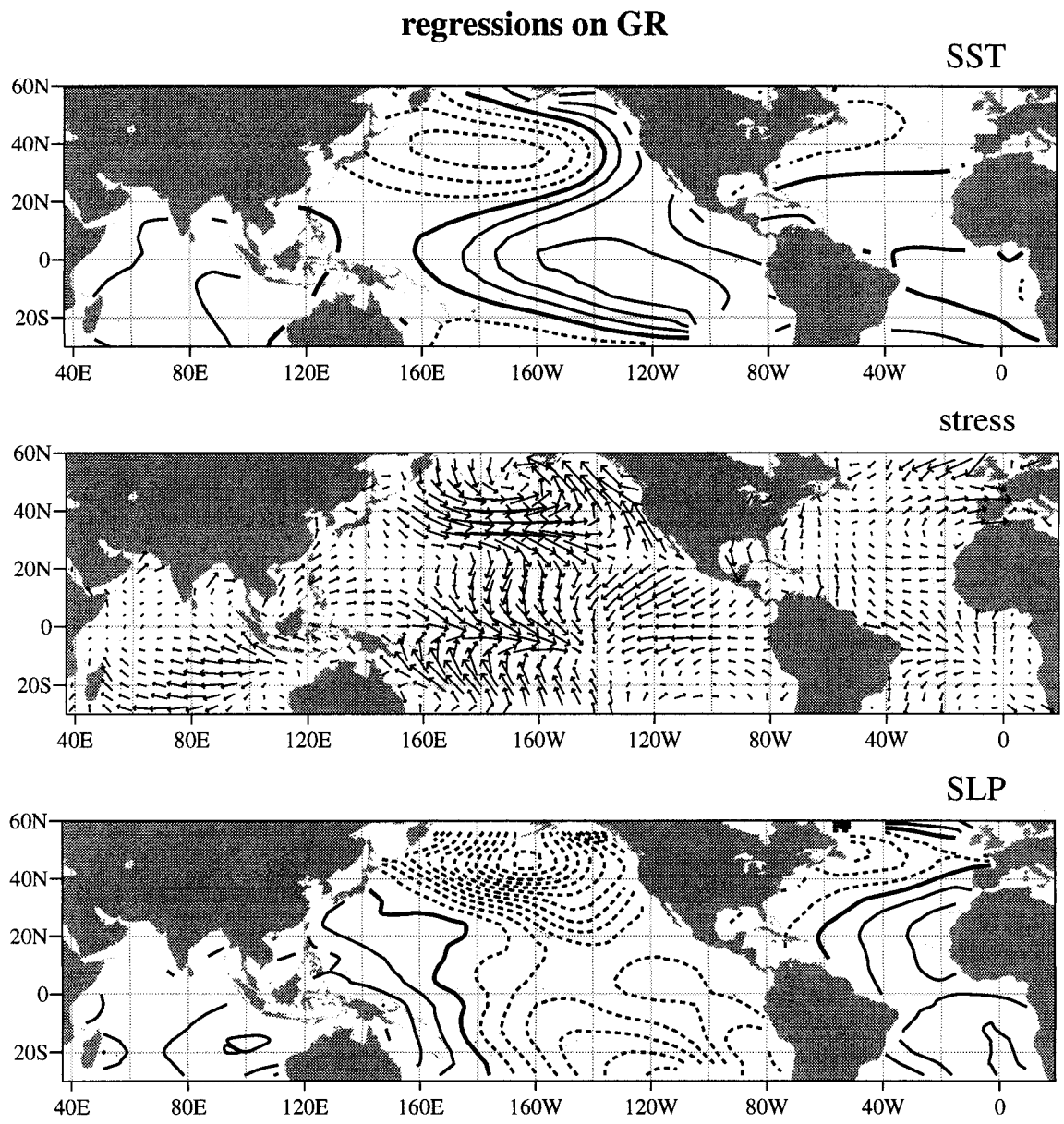


FIG. 4. Global fields regressed upon the monthly GR time series, displayed in Fig. 3: (a) SST, (b) wind stress, and (c) SLP. The contour interval is per unit standard deviation: (a) 0.1 K, (b) 8.3 $m^2 s^{-1}$ for the longest vector, and (c) 0.1 mb. Negative contours are dashed and the zero contour is thickened. Reproduced from Fig. 11 of Zhang et al. (1997).

nificantly on temperature but varies, to some extent, with precipitation at the nearby Gulkana and Anchorage stations.

With the exception of Wolverine, there is no statistically significant relationship between local wintertime temperature and precipitation for the Alaskan stations (not shown); at Wolverine, the correlation is positive. Yet temperatures at all three stations are significantly correlated with the wintertime streamflow of the Kenai River (ranging between 0.60 and 0.76). Among the three stations, only at Wolverine is the record of precipitation significantly correlated (0.77) with the streamflow of the Kenai River.

For three of the six glaciers, NSB is negatively correlated with summertime temperature at nearby stations. The relationship is usually most robust for stations that are closest to the glacier. For all six glaciers, there are no statistically significant correlations between NSB and summertime precipitation anomalies.

The correlations between NAB and temperature and precipitation at nearby stations replicate closely the correlations between NWB and winter temperature and pre-

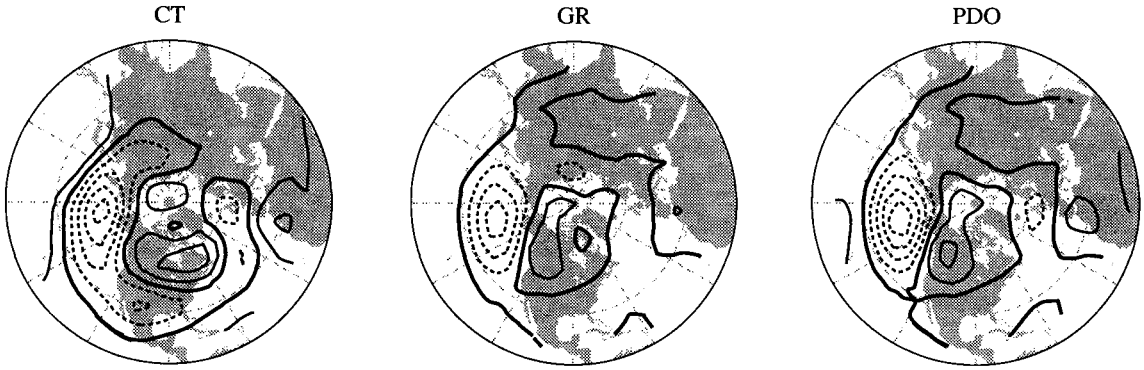


FIG. 5. 500-mb height anomalies regressed on the CT, GR, and PDO indexes from Fig. 3. The contour interval is 10 m per unit standard deviation of the index.

cipitation. Only at Gulkana is the correlation between NAB and summer temperature greater than that between NAB and winter precipitation. Hence our results agree with the previous findings: for maritime glaciers, the NAB is more strongly dependent on the local winter climate (precipitation in particular), while continental glaciers are mainly affected by summer temperature anomalies.

### *b. Atmospheric circulation and NWB*

We next identify the anomalies in the large-scale atmospheric circulation that are associated with the anomalies in the NWB at the Washington–Canadian glaciers and at the Wolverine glacier. The 500-mb geopotential heights ($Z_{500}$) are composited for extreme NWB years, where ''extreme'' is defined as one standard deviation above or below the mean. The composite associated with the Washington–British Columbia glaciers (the southern group) is formed using the South Cascade glacier record, chosen among the Washington–Canadian glaciers because the mass balance record is the longest at this site. Circles in Fig. 2 indicate the extreme years used in constructing the composites. We do not base composites on all of the mass balance data because the common overlap of the measurements is short. However, all of the cross correlations for the southern glaciers are positive and statistically significant (ranging from 0.53 to 0.87; see, e.g., Hodge et al. 1998). Hence, the South Cascade glacier should be a good representative for the maritime glaciers in Washington and southern British Columbia.

TABLE 3. Correlation of South Cascade mass balance and meteorological data for (top) winter and (bottom) summer. Winter (summer) average is defined as an average over Nov–Apr (May–Oct). Precipitation at Stampede Pass, Stevens Pass, and Paradise is limited to snow and ice (summed from measurements of daily accumulation), while at Seattle and Quillayute precipitation includes both liquid and solid forms. Correlations significant at the 5% level are shown in bold, where estimates for the number of degrees of freedom for correlations between time series with different decorrelation timescales as described in Bretherton et al. (1999). The NSB and NAB of the South Cascade glacier are not significantly correlated with summer precipitation at the stations nearby.

| | | NWB | NAB |
|---|---|---|---|
| Winter temperature | Seattle | **−0.43** | **−0.41** |
| | Quillayute | **−0.62** | **−0.54** |
| | Stampede | **−0.49** | **−0.44** |
| | Stevens | −0.38 | −0.39 |
| | Paradise | **−0.48** | **−0.43** |
| Winter precipitation | Seattle | **0.66** | **0.53** |
| | Quillayute | **0.63** | **0.58** |
| | Stampede | **0.69** | **0.62** |
| | Stevens | **0.70** | **0.64** |
| | Paradise | **0.76** | **0.65** |
| Summer temperature | Seattle | **−0.71** | **−0.47** |
| | Quillayute | **−0.58** | −0.09 |
| | Stampede | **−0.77** | **−0.46** |
| | Stevens | **−0.71** | **−0.58** |
| | Paradise | **−0.52** | 0.02 |

Composites of wintertime $Z_{500}$ (Fig. 6) and $Z_{500}$ anomalies (Fig. 7) show the low-frequency atmospheric circulations that correspond to extreme NWB years. There is some evidence for an inverse relationship between the patterns that produce extreme NWB years at South Cascade and Wolverine as seen in Fig. 8 or by comparing the patterns diagonal to one another in Fig. 7. Indeed, the correlation coefficient for NWB at the South Cascade and Wolverine glaciers is −0.56. Also of note is the nonlinear nature of the extremes. For example, the patterns associated with the high NWB at South Cascade and low NWB at Wolverine (Figs. 7a,d) indicate that the centers of action over northern Canada and in the North Pacific are of comparable amplitude. In contrast, Figs. 7b and 7c indicate the anomalies in the North Pacific are twice as large as those in northern Canada.

High NWB years at South Cascade occur when the 500-mb jet is well situated to bring offshore flow into the state of Washington (Fig. 6a). The $Z_{500}$ anomaly map (Fig. 7a) indicates that this brings an anomalous northwesterly flow and unusually cold conditions into Washington during years of high NWB (see also McCabe and

TABLE 4. As in Table 3, but for the Canadian glaciers with the temperature and precipitation from stations nearby. The NSB and NAB for the Canadian glaciers are not significantly correlated with summer precipitation at the stations nearby.

| | | NWB | | | NAB | | |
|---|---|---|---|---|---|---|---|
| | | Sentinel | Place | Peyto | Sentinel | Place | Peyto |
| Winter temperature | Vancouver | 0.01 | 0.05 | −0.38 | 0.11 | −0.02 | −0.16 |
| | Shalalth | 0.02 | 0.02 | −0.22 | 0.06 | 0.03 | 0.04 |
| | Calgary | −0.22 | −0.17 | **−0.53** | −0.01 | −0.16 | −0.18 |
| | Jasper | −0.20 | −0.12 | **−0.46** | −0.04 | −0.11 | −0.15 |
| Winter precipitation | Vancouver | **0.60** | **0.45** | 0.19 | **0.70** | 0.41 | 0.13 |
| | Shalalth | **0.65** | **0.74** | **0.48** | **0.69** | **0.71** | **0.46** |
| | Calgary | **0.49** | **0.42** | 0.43 | 0.32 | 0.40 | 0.20 |
| | Jasper | **0.49** | **0.52** | **0.53** | 0.33 | 0.39 | 0.39 |
| | | NSB | | | NAB | | |
| | | Sentinel | Place | Peyto | Sentinel | Place | Peyto |
| Summer temperature | Vancouver | −0.35 | **−0.64** | −0.21 | −0.32 | **−0.45** | −0.24 |
| | Shalalth | **−0.64** | **−0.61** | −0.39 | −0.52 | **−0.51** | −0.15 |
| | Calgary | −0.10 | −0.33 | −0.20 | −0.08 | −0.28 | −0.33 |
| | Jasper | −0.40 | **−0.52** | −0.40 | −0.25 | −0.39 | −0.38 |

Fountain 1995). The $Z_{500}$ composite for low NWB years at Wolverine is similar to that for high NWB years at South Cascade, which is reminiscent of the seesaw in NWB discussed by Walters and Meier (1989). High NWB years at Wolverine occur when the 500-mb jet is diverted away from the west coast of North America (Fig. 6b) by anomalously high pressure centered over Alberta, Canada (Fig. 7b). This circulation allows for anomalous southerly flow into the southern coast of Alaska, bringing with it anomalously warm and moist air.

Composites of $Z_{500}$ anomalies for the high Wolverine NWB and low South Cascade NWB (Figs. 7b,c) resemble the PNA pattern. The composites for high South Cascade NWB and low Wolverine NWB (Figs. 7a,d) bear less resemblance to an inverse PNA structure: the North America pressure anomalies are too severe relative to the Aleutian pressure anomalies and the structures are too zonal.

Maps of the difference in storminess for high minus low NWB years are composited in Fig. 9. This figure clearly shows that variations in the storminess stem from a displacement of the North Pacific storm track position. A displacement northward, toward Washington and Alaska, is associated with high NWB at South Cascade glacier, while anomalously high NWB at Wolverine glacier is associated with a southward displacement of the storm track *away* from Alaska and Washington and, hence, reduced storminess at high latitude.

### *c. Summary and discussion of the control of NWB and NAB at the glaciers of Washington, western Canada, and Alaska*

The relationship between the anomalies in the mass balance of these six glaciers and the seasonal anomalies in local temperature and precipitation reported in section

TABLE 5. As in Table 3, but for the Wolverine and Gulkana glaciers with the winter averaged temperature and precipitation at selected sites in southern Alaska. We include winter–spring (Nov–Jun) streamflow from the Kenai River to supplement the information about precipitation. The NSB and NAB for the Alaskan glaciers are not significantly correlated with summer precipitation at the stations nearby.

| | | NWB | | NAB | |
|---|---|---|---|---|---|
| | | Wolverine | Gulkana | Wolverine | Gulkana |
| Winter temperature | Anchorage | **0.70** | 0.10 | **0.60** | 0.05 |
| | Wolverine | **0.63** | −0.01 | 0.45 | 0.12 |
| | Gulkana | **0.69** | 0.18 | **0.63** | 0.10 |
| Winter precipitation | Anchorage | 0.05 | **0.44** | −0.05 | 0.02 |
| | Wolverine | **0.81** | −0.01 | **0.86** | 0.30 |
| | Gulkana | −0.18 | **0.54** | −0.33 | −0.21 |
| Winter spring streamflow | Kenai | **0.80** | 0.14 | **0.65** | 0.28 |
| | | NSB | | NAB | |
| | | Wolverine | Gulkana | Wolverine | Gulkana |
| Summer temperature | Anchorage | −0.42 | **−0.52** | −0.09 | **−0.54** |
| | Wolverine | **−0.60** | **−0.79** | −0.35 | **−0.78** |
| | Gulkana | −0.47 | **−0.74** | −0.32 | **−0.75** |

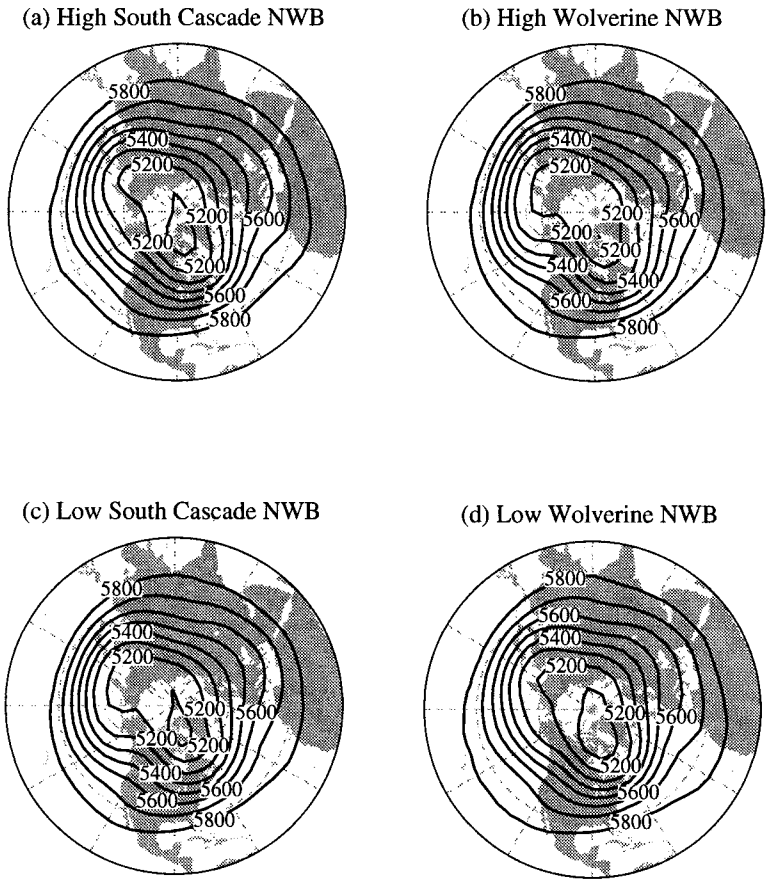


FIG. 6. Composites of winter (NDJFMA) mean 500-mb height when the glacier NWB is greater than one standard deviation above (top) and below (bottom) the mean for South Cascade (left) and Wolverine (right) glaciers.

3a are summarized schematically in Fig. 1; they confirm and extend the findings from other studies (e.g., Letréguilly 1988; Walters and Meier 1989; Mayo and March 1990). Anomalies in the NWB and NAB for all but Gulkana glacier are positively correlated with local winter precipitation anomalies. NWB and NAB anomalies for the glaciers in the southern group have weak correlations with local winter temperature anomalies that are either negative or insignificant. In contrast, anomalies in the NWB and NAB at the Wolverine glacier in Alaska have strong *positive* correlations with winter temperature anomalies. Unlike the maritime glaciers, the anomalies of the NAB of the Gulkana glacier, located far inland in Alaska, is regulated mainly by summer temperature anomalies. All glaciers experience more net summer melt (negative NSB anomalies) with higher temperatures, but NSB is not correlated with local summer precipitation at any of the glaciers.

The seasonal circulation anomaly pattern associated with the glacier mass balance anomalies is the PNA, consistent with the results of Walters and Meier (1989). The PNA is prominent for the mass balance anomalies because the PNA is associated with changes in the local weather variables (Yarnal and Diaz 1986; Cayan and Peterson 1989) that are paramount to the changes in the mass balance of the glaciers in Washington, western Canada, and Alaska.

Previous investigators have hypothesized that a positive correlation exists between NWB and storminess (e.g., McCabe and Fountain 1995). Our results indicate that positive anomalies in the mass balance of the South Cascade glacier are indeed associated with more storminess (section 3a). However, high NWB at Wolverine is associated with *less* storminess (Fig. 9) and a deeper low that has moved westward, out of the Gulf of Alaska and into the North Pacific (Fig. 7b).[3] When GR is regressed upon the product of the monthly mean flow and the monthly mean moisture (Fig. 10), it is clear that positive GR leads to an enhanced moisture flux into this region and to positive anomalies in the moisture flux convergence, probably due to the coastal orography.

[3] Our findings contradict the notion that a deeper Aleutian low is concomitant with a northward displacement of the storm track (Yarnal and Diaz 1986; Cayan and Peterson 1989).

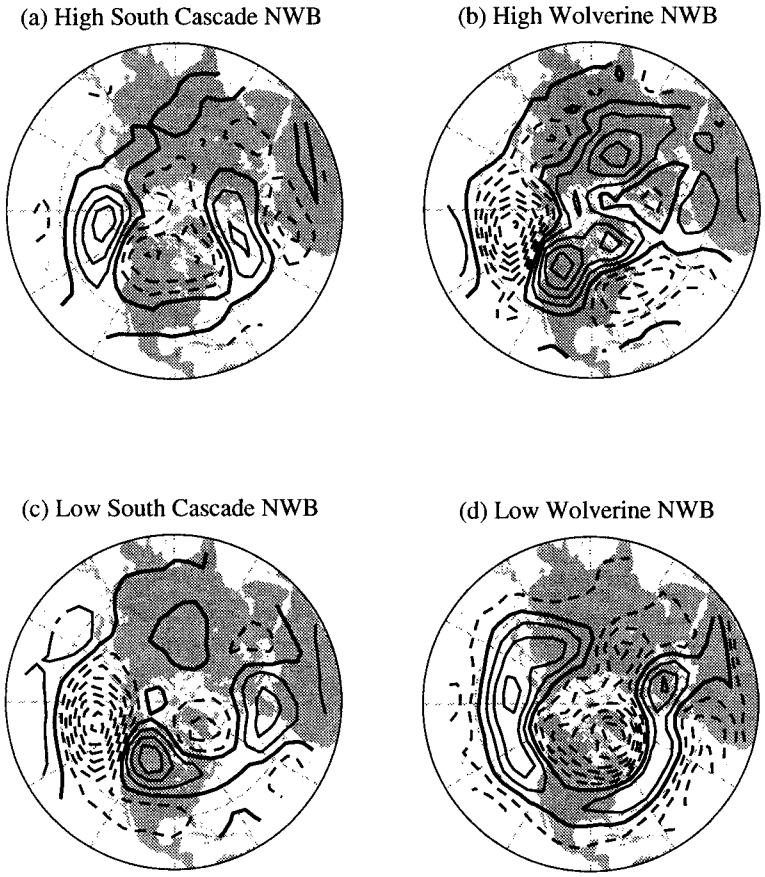


FIG. 7. As in Fig. 6, but the composites are 500-mb height anomalies, where anomalies are defined as departures from the climatological mean. The contour interval is 10 m.

Hence, any decrease in precipitation at Wolverine associated with a decrease in storminess is, apparently, more than compensated by an increase in the moisture convergence due to changes in the seasonal mean circulation anomaly. In contrast, when CT is regressed on the vertically integrated moisture convergence, the pattern of anomalies in the Gulf of Alaska is similar to that in Fig. 10, but the amplitude is only half that associated with GR. This pattern is consistent with the weaker relationship between CT and NWB at Wolverine.

Previous studies have reported that the NWB of the maritime Alaskan glaciers has an out-of-phase relationship with the NWB of the maritime glaciers in the southern group. This relationship is clearly supported by the

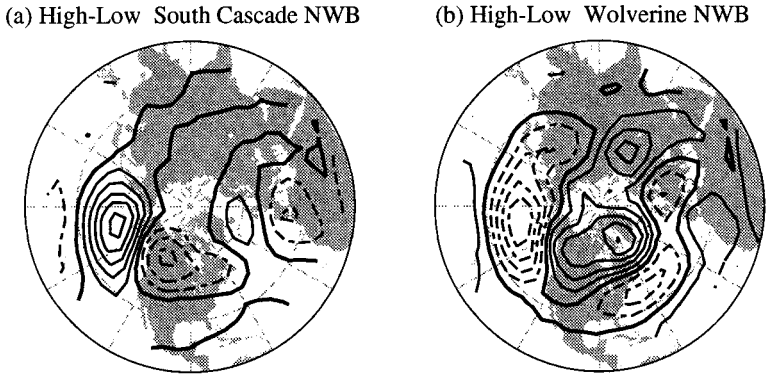


FIG. 8. Difference between composites from Fig. 7. The contour interval is 20 m.

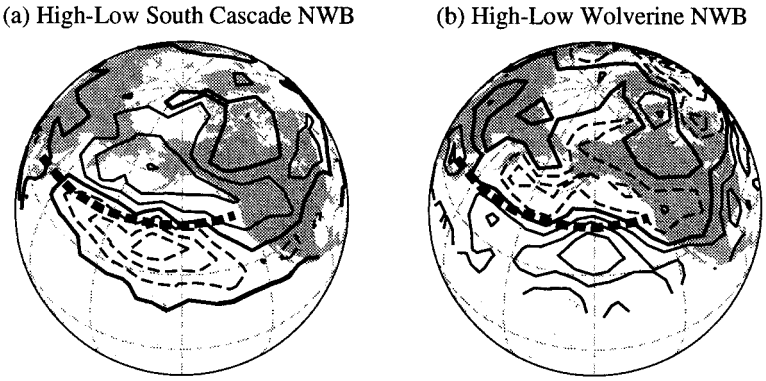


FIG. 9. Composite difference in storminess (defined as the rms of high-passed $Z_{500}$ anomalies) for the high minus low years for the South Cascade and Wolverine glaciers. Climatological wintertime jet (maximum storminess in meridional direction) is shown by heavy dashed line. The contour interval is 3 m.

similarity in the patterns of the $Z_{500}$ anomalies during the years of opposite NWB extremes at Wolverine and South Cascade glaciers (Fig. 7) and the antisymmetric storminess patterns associated with high NWB at the Wolverine and South Cascade glaciers (Fig. 9). In the next sections, we discuss the global nature of these regional climate anomalies.

## 4. The large-scale atmosphere–ocean circulation anomalies and wintertime glacier mass balance

We now determine how the mass balance of the six glaciers is affected by the interannual ENSO phenomenon and the decadal ENSO-like variability. The state of these two climate phenomena is indicated by the CT and GR indexes, respectively. We will also use the PDO time series defined by Mantua et al. (1997), which is related to both the GR and CT indexes (see sections 2 and 5).

Figure 3 shows the time series of the three climate indexes: CT, GR, and PDO. Table 6 summarizes the correlations between NWB and the three climate indexes. The strongest correlations between NWB and these indices are for PDO, with GR following close behind. None of the correlations between the climate indexes and NWB at Gulkana or Sentinel is significant.[4,5]

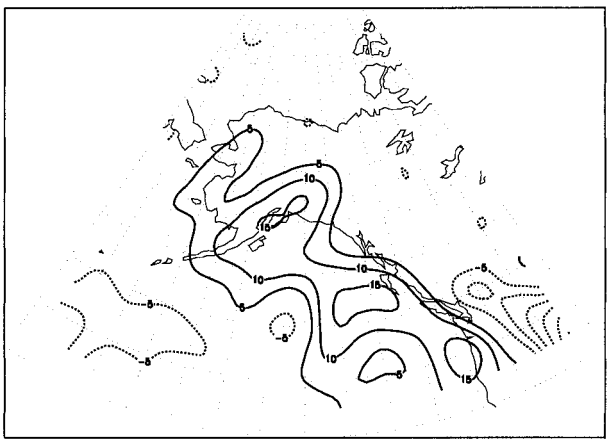

FIG. 10. Regression of GR on the convergence of the vertically integrated moisture flux. Moisture flux is calculated as the product of monthly mean velocity and monthly mean specific humidity. Units are $10^{-7}$g kg$^{-1}$ s$^{-1}$ per unit standard deviation of GR. Calculations and figure made by R. Garreaud.

### a. The GR–PDO (ENSO-like) atmosphere–ocean phenomenon and the glacier mass balance

The PDO and GR indices are positively correlated with the Alaskan maritime Wolverine glacier and negatively correlated with three out of four of the glaciers in the southern group (Table 6). The variance of NWB associated with PDO (GR) anomaly patterns is up to 56% (35%) of the total variance of the NWB. The reason the GR and PDO climate anomalies are more influential than ENSO (CT) for the mass balance anomalies of the Alaskan Wolverine glacier is suggested by comparing the midlatitude circulation anomalies associated with these three climate indexes (Fig. 5) to those that are associated with anomalies in the mass balance of the glaciers (Fig. 7). Recall that the NWB of the Wolverine glacier is positively correlated with local temperature and precipitation (section 3a). The $Z_{500}$ anomaly patterns associated with positive GR (or PDO) and positive anomalies in glacier mass balance at Wolverine suggest

[4] The low correlations at Sentinel in Table 6 may be due to relatively high uncertainties in the measured mass balance at this glacier (R. D. Moore 1998, personal communication).

[5] Peyto NWB is strongly correlated with GR and PDO, suggesting Peyto may have a closer relationship with Pacific maritime climate than previously thought.

TABLE 6. Correlation of wintertime (Nov–Apr) mean climate indexes and (top) NWB or (bottom) NAB. Correlations between NSB and the same climate indices (not shown) are not significant. Statistical convention as in previous tables. The climate indexes are defined in section 3 and have been adopted from previous studies.

| NWB | GR | PDO | CT |
|---|---|---|---|
| South Cascade | **−0.53** | **−0.75** | **−0.43** |
| Sentinel | −0.36 | −0.39 | −0.10 |
| Place | **−0.46** | **−0.47** | −0.19 |
| Peyto | **−0.59** | **−0.74** | −0.35 |
| Wolverine | **0.58** | **0.71** | 0.23 |
| Gulkana | 0.30 | 0.13 | −0.10 |
| **NAB** | **GR** | **PDO** | **CT** |
| South Cascade | **−0.49** | **−0.65** | **−0.45** |
| Sentinel | −0.30 | −0.28 | −0.05 |
| Place | **−0.49** | −0.39 | −0.04 |
| Peyto | **−0.46** | −0.40 | −0.08 |
| Wolverine | **0.55** | **0.68** | 0.37 |
| Gulkana | 0.27 | 0.26 | 0.18 |

a more maritime (southerly) trajectory from the ocean compared to the $Z_{500}$ anomaly pattern associated with CT (ENSO). The more southerly flow brings more anomalously warm, moist air and greater moisture flux convergence into the region by the seasonal mean circulation (not shown), which is reflected in the increased mass balance and streamflow anomalies, despite the reduction in storminess (see Figs. 7 and 9).

The mass balance of the South Cascade glacier is negatively correlated with the GR and PDO time series (Table 6). The circulation anomalies associated with these time series (Fig. 5) indicate that during a positive GR anomaly there is a reduction in the onshore flow (the climatological westerlies). The $Z_{500}$ anomaly patterns associated with positive GR and low mass balance for the South Cascade indicate the presence of anomalously warm air over the region, consistent with the negative local relationship between temperature and NWB at the South Cascade glacier (Table 3). However, the NWB for the South Cascade and the southern glacier group is more affected by precipitation than by temperature (see Tables 3 and 4). Hence, to understand the relationship between the mass balance of these glaciers and the large-scale climate anomalies, we next examine the relationship between wintertime storminess and the climate indexes.

The correlation maps for wintertime storminess with the three winter mean climate indices are displayed in Fig. 11. Storminess anomalies associated with ENSO are mainly limited to the the subtropical Pacific (Fig. 11a). In contrast, the decadal ENSO-like variability (GR) is associated with fluctuations in the storminess in the midlatitude and subpolar northeast Pacific (Fig. 11b). The correlation between storminess and the PDO appears to be an amalgamation of the storminess anomalies associated with the GR and CT indexes (cf. Figs. 11a,b with 11c), and this is to be expected (the correlations between the winter mean PDO index and the GR and CT indexes are 0.73 and 0.30, respectively).

The patterns of storminess anomalies associated with NWB anomalies at Wolverine and South Cascade glaciers that are shown in Fig. 9 are very similar to those associated with the decadal ENSO-like phenomena, as indicated by the correlation maps between storminess and the GR or PDO indexes (Figs. 11b,c). Throughout the maritime region extending from southern Oregon to northwestern Alaska there is a decrease in storminess associated with positive GR and PDO anomalies. The reduction in storminess during low NWB years for the southern glacier group is consistent with precipitation being the dominant variable controlling the NWB of the southern glacier group. The GR and PDO are highly correlated with the NWB of the southern group because of this strong relationship between NWB and precipitation. The analysis of Wolverine glacier NWB and the local climate variables is consistent with the negative relationship between GR and storminess in maritime Alaska, which together signal an *enhancement* in NWB at Wolverine because the reduction in storminess is more than compensated by the anomalous southerly advection of warmer, more moist air from the south, leading to positive snowfall anomalies.

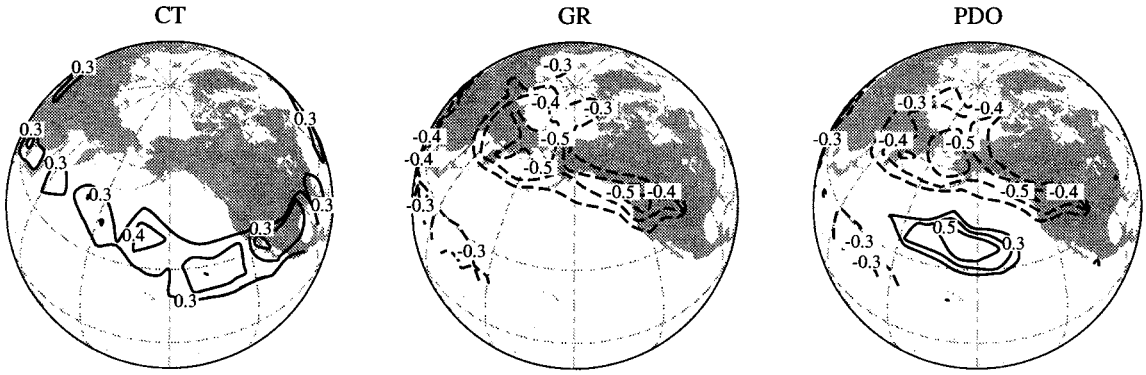


FIG. 11. Correlation maps of winter (NDJFMA) mean storminess with winter mean climate indexes for the period of record 1947–94. Contours show correlations that exceed the 95% confidence level where each year is considered to be independent of the last. Positive correlations indicate more storminess associated with warmer water in the tropical Pacific and colder water in the North Pacific.

*b. ENSO and the glacier mass balance*

For all six glaciers examined, correlations between NWB and CT are much weaker than between NWB and PDO or GR. About 20% of the variance of the South Cascade NWB is associated with ENSO (see last column of Table 6). Otherwise, ENSO is seen to have no statistically significant impact on the other five glaciers. Note, because there is at best a very weak relationship between ENSO and precipitation in the Pacific Northwest (Ropelewski and Halpert 1987), the significant negative correlation of ENSO with ostreamflow(Cayan and Webb 1992) and snowpack (Cayan 1996) in the Cascade Mountains and with the NWB of the South Cascade glacier are primarily determined by temperature changes that affect winter melt.

Why is the relationship between ENSO and the NWB of these glaciers so weak? Recall that the NWB of the southern group of glaciers was found to be most highly correlated with local precipitation anomalies, having only a weak (South Cascade and Peyto) or no (Sentinel and Place) correlation with wintertime temperature. The importance of precipitation for the NWB of the southern group is shown in the composites of local storminess anomalies found during extreme NWB years in the southern glaciers (Fig. 10). However, Fig. 11 indicates that ENSO has no significant effect on storminess north of central California; hence, ENSO contributes very little to the mass balance of the southern group of glaciers. The crucial element for regulating the NWB of the Wolverine glacier is the southerly flow of moist maritime air (Fig. 7). Though the seasonal mean circulation anomalies associated with GR and CT are only subtly different at $Z_{500}$ (Fig. 5), there are pronounced differences in the amplitude of the moisture advection into the region associated with GR and CT. ENSO has little effect on the Wolverine glacier because, when compared to GR, ENSO has a small effect on moisture flux convergence in the Gulf of Alaska by the low-frequency circulation.

*c. Comparison with previous results*

Previous investigators used the PNA and various indexes of ENSO as the launching point to examine the relationship between the large-scale climate anomalies and the mass balance of the glaciers in maritime Washington and western Canada and extending northward into Alaska (see discussion in section 1). In our complementary approach, we use the glacier mass balance data to identify the circulation anomalies that are important for the variability in the mass balance. We confirm the results of Walters and Meier (1989): the mass balance is strongly affected by a pattern of circulation anomalies in the midlatitudes that is very similar to the classic PNA pattern of Wallace and Gutzler (1981).

Walters and Meier (1989) suggested there may be a relationship between ENSO and the mass balance of the maritime glaciers in Washington and western Canada–Alaska *because* the PNA index (defined in Wallace and Gutzler 1981) is correlated with both the mass balance of these glaciers and with ENSO. Hodge et al. (1998) found ENSO was indeed weakly but positively (negatively) correlated with the mass balance of the Wolverine (South Cascade) glacier. Except for the South Cascade glacier, however, our results indicate that no statistically significant relationships exist between ENSO and the NWB or NAB of the glaciers in maritime Washington, southern British Columbia, and Alaska. Rather, we find that the mass balance anomalies are highly correlated with the GR time series, which represents the temporal evolution of a large-scale atmosphere–ocean climate anomaly whose pattern qualitatively resembles ENSO but is mostly realized on longer (decadal) timescales. The subtle but crucial differences in the midlatitude circulation anomalies associated with the ENSO (CT) and the ENSO-like (GR) phenomena [e.g., see Fig. 5 of Zhang et al. (1997)] explains why the latter is a substantial contributor to the NWB of these maritime glaciers and ENSO is not.

Our results concerning the decadal ENSO-like control of the NWB of the southern glaciers are consistent with the results of Moore and McKendry (1996), who examined the relationship between the British Columbia snowpack anomalies and the wintertime climate anomalies. Specifically, they noted an abrupt change in 1976 to a reduced snowpack in the far southern part of the province and suggested that this was likely due to less precipitation and/or more winter melt [due to warmer conditions; but cf. Moore (1996)]. Our results are also consistent with Gutzler and Rosen (1992), who found a strong positive correlation between snowpack in the U.S. Pacific Northwest and the PNA, and with those of Brown and Goodison (1996), who showed that the snowpack in southern British Columbia is better correlated with the PNA than with ENSO.

## 5. Discussion and implications

Our results show that the mass balance of the glaciers along maritime Washington, western Canada, and Alaska are strongly affected by a low-frequency (decadal) ENSO-like phenomenon, with time index GR (Fig. 3) and spatial structure shown in Figs. 4, 5b, and 11b. The percent of variance of NWB and NAB explained by the GR (PDO) time series is as high as 35% (56%) (Table 6).

The decadal ENSO-like phenomenon is clearly a coupled atmosphere–ocean phenomenon (Zhang et al. 1997); the GR time series shows that this phenomenon has a characteristic timescale of many years to decades. With its roots in the tropical Pacific, the circulation anomalies extend to the midlatitude Pacific in both hemispheres, with impacts across the Americas (Zhang et al. 1997; Mantua et al. 1997; R. Garreaud and D. Battisti 1999). The physics associated with this climate

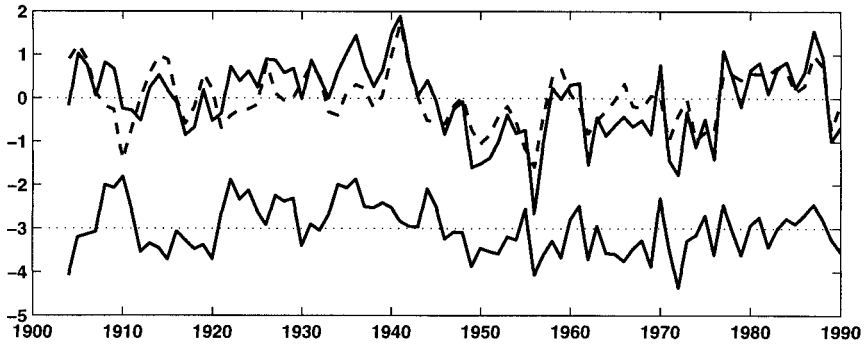


FIG. 12. The PDO time series [solid line; from Mantua et al. (1997)] and reconstructed PDO time series (dashed line) from the multilinear best fit to the PDO using the ENSO (CT) and ENSO-like (GR) indexes. The residual of these time series (PDO minus reconstructed PDO) is shifted by −3 for better visualization.

phenomenon is not yet known, though several hypotheses have been put forward and are being tested by the community. Nonetheless, the ocean must play a prominent role due to its high thermal inertia and long timescale for dynamical adjustment. Thus, it is reasonable to expect that, eventually, there will be some predictability of this phenomenon and its impacts. At that time, the strong relationship between this phenomenon and the mass balance of the maritime glaciers on the northeast Pacific rim can be exploited to make short-term climate forecasts of glacier mass balance and of the climate variables that control the glacier mass balance (e.g., storminess and precipitation anomalies in maritime Washington–western Canada and Alaska; temperature in maritime Alaska).

Though the GR and PDO time series are highly correlated, the variance of mass balance explained by PDO time series is greater than that explained by the GR. Indeed, the midlatitude circulation anomalies associated with the GR and PDO are very similar, and both contain the circulation and storminess anomalies that are important for the NWB of the glaciers along the maritime northwest coast of North America. However, it is unclear how much, if any, of the additional information on mass balance contained in the PDO (i.e., information not already contained in GR) is information that can be used for prediction (specifically, for prediction of mass balance).

In Fig. 12 we plot the PDO index and a reconstructed PDO index. The latter is the best fit to the PDO index using the CT and GR indexes and multiple linear regression; hence, the reconstructed PDO index is also the portion of the PDO that is *known* to be associated with low-frequency, coupled atmosphere–ocean phenomena. The reconstructed PDO explains 55% of the variance of the PDO index. Examination of Fig. 12 reveals that a substantial portion of the *residual* of these two time series is at interannual timescales (but not associated linearly with ENSO), particularly during the recent half-century. A portion of this residual might be due to a *midlatitude* atmosphere–ocean phenomenon in which the ocean dynamical response is crucial (e.g., Latif and Barnett 1994), and this portion of the residual would render further predictive skill for the PDO (hence, for the glacier mass balance) due to the long memory of the ocean. However, a portion of this residual is almost certainly due to a simple low-frequency enhancement of the natural atmospheric patterns of variability in the midlatitude North Pacific (in this case, the PNA) by local atmosphere–ocean thermal coupling in the midlatitudes and *without* active ocean dynamics (Frankignoul 1985; Barsugli 1995; Lau and Nath 1996; Barsugli and Battisti 1998). Because the PNA pattern is an internal *stochastic* mode of the atmosphere (e.g., Saravanan 1998), there is not likely to be any useful extra information in this component of the residual of the PDO index.

We hypothesize that at this time the combination of CT and GR provides predictive skill equivalent to that of the PDO for the South Cascade glacier. A multiple linear regression of CT and GR on the mass balance for South Cascade explains 40% and 36% of the variances of the NWB and NAB, respectively—about 12% more than GR explains alone. We compute the multiple regression for only the South Cascade glacier because CT does not explain a significant fraction of the variance of the mass balance on the other five glaciers.

More generally, since the glacier mass balance anomalies are strongly affected by the PNA and its attendant storminess and precipitation anomalies (section 3), information on the effect of anthropogenic forcing on the frequency and amplitude of the PNA pattern can be used to anticipate how anthropogenic forcing will affect both the mean and the variance of the mass balance of the maritime glaciers along the northwest coast of North America.

## 6. Conclusions

We examined the net winter, summer, and annual mass balance of six glaciers along the northwest coast of North America in Washington State and southwestern

Canada (the southern group) and Alaska, and we determined how mass balance is related to local weather anomalies and to large-scale atmosphere–ocean climate anomalies. The net winter (NWB) and net annual (NAB) mass balance anomalies for the maritime glaciers in the southern group are shown to have strong positive correlations with local wintertime precipitation anomalies and weak negative correlations with local temperature anomalies. The NWB and NAB of the maritime Wolverine glacier in Alaska are also positively correlated with local precipitation, but they are *positively* correlated with local winter temperature anomalies.

The NWB (NAB) of each of the glaciers in the southern group are negatively correlated with the NWB (NAB) of the Wolverine glacier in Alaska. The patterns of the wintertime 500-mb circulation and storminess anomalies associated with years of high NWB of the glaciers in the southern group are similar to those associated with low NWB of the Wolverine glacier in Alaska, and vice versa. The Aleutian and central Canadian lobes of the PNA are prominent in these patterns. The NWB and NAB of the glaciers in the southern group are anomalously low when there is less local winter storminess (defined as the high-passed $Z_{500}$ anomalies) and thus less local precipitation. In contrast, positive anomalies in the NWB and NAB of the Wolverine glacier are associated with less storminess because there is a concomitant increase in warm, moist air being advected into the region by the anomalies in the averaged wintertime circulation, yielding net positive snowfall anomalies due to increases in the moisture convergence associated with the orographic lifting of the onshore flow.

There are two prominent, pan-Pacific, coupled atmosphere–ocean phenomena: the interannual ENSO phenomenon, and a climate phenomenon that has a footprint on the ocean and atmosphere that is similar to ENSO but shows mainly decadal-scale variability with some rapid interannual ''jumps'' (e.g., about 1975). The decadal ENSO-like climate phenomenon is shown to have a large impact on the NWB and NAB of these maritime glaciers, accounting for up to 35% of the variance in NWB. The patterns of 500-mb circulation and storminess anomalies associated with the decadal ENSO-like mode resemble the PNA pattern and are very similar to those associated with the years of extreme NWB on the glaciers in both the southern group and on the Wolverine glacier. Hence, the decadal mode affects the local precipitation, which is most crucial for the NWB for these maritime glaciers, because it strongly affects the storminess over southern British Columbia and Washington and the moisture transported by the seasonally averaged circulation into maritime Alaska. In contrast, ENSO is only weakly related to the NWB of these glaciers because (i) the large-scale circulation anomalies associated with ENSO do not produce substantial anomalies in moisture advection into Alaska, and (ii) the storminess and precipitation anomalies associated with ENSO are far to the south of the southern glacier group.

*Acknowledgments.* We thank Howard Conway, Al Rasmussen, and Charlie Raymond for helpful discussion, especially concerning the glacier data, and Nate Mantua for providing the PDO and CT indexes and discussions about climate–hydrologic relationships. We thank Rene Garreaud for performing the regressions of moisture flux convergence upon the CT and GR indexes. We thank Chris Bretherton for helping us determine the appropriate number of degrees of freedom for correlations between time series with different decorrelation timescales. This work was supported by a grant from the National Science Foundation (ATM-9530691).

## REFERENCES

Barsugli, J. J., 1995: Idealized models of intrinsic midlatitude atmosphere–ocean interaction. Ph.D. thesis, University of Washington, 189 pp. [Available from UMI, 300 Zeeb Rd., Ann Arbor, MI 48106.]

——, and D. S. Battisti, 1998: The basic effects of atmosphere–ocean thermal coupling on midlatitude variability. *J. Atmos. Sci.,* **55,** 477–493.

Bretherton, C. S., M. Widmann, V. P. Dymnidov, J. M. Wallace, and I. Blade, 1999: The effective number of spatial degrees of freedom of a time-varying field. *J. Climate,* **12,** 1990–2009.

Brown, R. D., and B. E. Goodison, 1996: Interannual variability in reconstructed Canadian snow cover, 1915–1992. *J. Climate,* **9,** 1299–1318.

Cayan, D. R., 1996: Interannual climate variability and snowpack in the western United States. *J. Climate,* **9,** 928–948.

——, and D. H. Peterson, 1989: The influence of North Pacific atmospheric circulation on the streamflow in the west. *Aspects of Climate Variability in the Pacific and Western Americas, Geophys. Monogr.,* No. 55, Amer. Geophys. Union, 375–397.

——, and R. H. Webb, 1992: El Niño/Southern Oscillation and streamflow in the western United States. *El Niño: Historical and Paleoclimatic Aspects of the Southern Oscillation,* H. F. Diaz and V. Markgraf, Eds., Vol. 44, Cambridge University Press, 29–68.

Demuth, M. N., and R. Keller, 1997: An assessment of the mass balance of Peyto Glacier (1966–1995) and its relation to recent and past-century climatic variability. Tech. Rep., National Hydrology Research Institute Contribution Series CS-97007, 45 pp. [Available from Environment Canada, 11 Inovation Blvd., Saskatoon, SK S7N 3H6, Canada.]

Deser, C., and J. M. Wallace, 1990: Large-scale atmospheric circulation features of warm and cold episodes in the tropical Pacific. *J. Climate,* **3,** 1254–1281.

Frankignoul, C., 1985: Sea surface temperature anomalies, planetary waves, and air–sea feedback in the middle latitudes. *Rev. Geophys.,* **23,** 357–390.

Garreaud, R., and D. S. Battisti, 1999: ENSO-like interannual to decadal variability in the Southern Hemisphere. *J. Climate,* **12,** 2113–2123.

Gutzler, D. S., and R. D. Rosen, 1992: Interannual variability of wintertime snow cover across the Northern Hemisphere. *J. Climate,* **5,** 1441–1447.

Hodge, S. M., D. C. Trabant, R. M. Krimmel, T. A. Heinrichs, R. S. March, and E. G. Josberger, 1998: Climate variations and changes in mass of three glaciers in western North America. *J. Climate,* **11,** 2161–2179.

Horel, J. D., and J. M. Wallace, 1981: Planetary-scale atmospheric phenomenon associated with the Southern Oscillation. *Mon. Wea. Rev.,* **109,** 813–829.

IAHS (ICSI)/UNEP/UNESCO, 1993: *Fluctuations of Glaciers, 1985–1990*. W. Haberli and M. Hoelzle, Eds., Vol. 6, World Glacier Monitoring Service, 322 pp.

——, 1996: *Glacier Mass Balance Bulletin No. 4, 1994–1995.* W. Haberli, M. Hoelzle, and S. Suter, Eds., World Glacier Monitoring Service, 90 pp.

Karl, T. R., C. N. Williams Jr., and F. T. Quinlan, 1990: United States Historical Climatology Network (HCN) serial temperature and precipitation data. Tech. Rep. NDP-019/R1, Carbon Dioxide Information Analysis Center, Oak Ridge National Laboratory, 274 pp. [Available from Oak Ridge National Laboratory, P. O. Box 2008, Oak Ridge, TN 37831.]

Kushnir, Y., and J. M. Wallace, 1989: Low-frequency variability in the Northern Hemisphere winter: Geographical distribution, structure and time-scale dependence. *J. Atmos. Sci.,* **46,** 3122–3142.

Latif, M., and T. Barnett, 1994: Causes of decadal climate variability over the North Pacific and North America. *Science,* **266,** 634–637.

Lau, N.-C., and M. J. Nath, 1996: The role of the atmospheric bridge in linking tropical Pacific ENSO events to extratropical SST anomalies. *J. Climate,* **9,** 2036–2057.

Letréguilly, A., 1988: Relation between the mass balance of western Canadian mountain glaciers and meteorological data. *J. Glaciol.,* **34,** 11–18.

Mantua, N. J., S. R. Hare, Y. Zhang, J. M. Wallace, and R. C. Francis, 1997: A Pacific interdecadal climate oscillation with impact on salmon production. *Bull. Amer. Meteor. Soc.,* **78,** 1–11.

Mayo, L. R., and D. Trabant, 1984: Observed and predicted effects of climate change on Wolverine Glacier, Southern Alaska. *Proc. The Potential Effects of Carbon Dioxide-Induced Climate Change in Alaska,* University of Alaska, 114–123.

——, and R. S. March, 1990: Air temperature and precipitation at Wolverine Glacier, Alaska: Glacier growth in a warmer, wetter climate. *Ann. Glaciol.,* **14,** 191–194.

McCabe, G. J., and A. Fountain, 1995: Relations between atmospheric circulation and mass balance of South Cascade Glacier. *Arct. Alp. Res.,* **27,** 226–233.

Moore, R. D., 1996: Snowpack and runoff responses to climatic variability, southern coast mountains, British Columbia. *Northwest Sci.,* **70,** 321–333.

——, and I. G. McKendry, 1996: Spring snowpack anomaly patterns and winter climatic variability, British Columbia, Canada. *Water Resour. Res.,* **32,** 623–632.

Reynolds, R. W., and T. M. Smith, 1995: A high-resolution global sea surface temperature climatology. *J. Climate,* **8,** 1571–1583.

Rogers, J. C., 1997: North Atlantic storm track variability and its association to the North Atlantic Oscillation and climate variability of northern Europe. *J. Climate,* **10,** 1635–1647.

Ropelewski, C. F., and M. S. Halpert, 1987: Global and regional scale precipitation patterns associated with the El Niño/Southern Oscillation. *Mon. Wea. Rev.,* **115,** 1606–1626.

Saravanan, R., 1998: Atmospheric low-frequency variability and its relationship to midlatitude SST variability: Studies using the NCAR Climate System Model. *J. Climate,* **11,** 1386–1404.

Wallace, J. M., and D. S. Gutzler, 1981: Teleconnections in the geopotential height field during the Northern Hemisphere winter. *Mon. Wea. Rev.,* **109,** 784–812.

Walters, R. A., and M. F. Meier, 1989: Variability of glaciers mass balances in western North America. *Aspects of Climate Variability in the Pacific and Western Americas, Geophys. Monogr.,* No. 55, Amer. Geophys. Union, 365–374.

Yarnal, B., 1984: Relationships between synoptic-scale atmospheric circulation and glacier mass balance in south-western Canada during the International Hydroloogical Decade, 1965–74. *J. Glaciol.,* **30,** 188–198.

——, and H. F. Diaz, 1986: Relationships between extremes of the Southern Oscillation and the winter climate of the Anglo-American Pacific coast. *J. Climatol.,* **6,** 197–219.

Zhang, Y., J. M. Wallace, and D. S. Battisti, 1997: ENSO-like interdecadal variability: 1900–93. *J. Climate,* **10,** 1004–1020.